D34

N79-24035

ELECTRIC FIELDS IN IRRADIATED DIELECTRICS

A. R. Frederickson
Rome Air Development Center

ABSTRACT

An existing model for quantitatively predicting electric field build-up in dielectrics is used to demonstrate the importance of material parameters. Results indicate that electron irradiation will produce 10^6 V/cm in important materials. Parameters which can alter this build-up are discussed. Comparison to known irradiation induced dielectric charging experiments is discussed.

INTRODUCTION

We wish to discuss the situation where space radiation penetrates a dielectric surface producing internal charge densities, fields, and possible breakdown effects. There are negligible transient magnetic field effects under typical space irradiation which corresponds to the classical dielectric work under low intensity laboratory irradiations. It has long been known that dielectrics can be made to spontaneously breakdown (discharge) under such irradiations (refs. 1,2) and that breakdown may occur during or hours after cessation of the irradiation (ref. 3). The Lichtenberg figures (ref. 1) which often result from such discharges are clear indications that internal bulk processes are fundamentally involved in the discharges. Work with samples which have not discharged indicates that very large (10^6 V/cm) fields are often generated in irradiated dielectrics (refs. 4 to 6). We will apply recently developed (refs. 7,8) methodology to calculate the internal electric fields, charge densities and current densities for irradiated dielectrics under such laboratory irradiations. In principle the method can be used for space radiations but the necessary set of parameters has not yet been quantitatively evaluated for space radiation.

The Lichtenberg figure effect is so dramatic that it has long been of interest and results of work on the effect may be helpful to the spacecraft charging area. The effect is usually reported for electron irradiations above 100 keV but has also been seen for X-rays. The figures are often associated with a large physical flaw in the sample introduced either prior to or after the irradiation. Discharges in materials do not always produce figures. Samples with initial figures can produce further Lichtenberg figures upon subsequent additional irradiations. We therefore deduce that spacecraft dielectrics may discharge spontaneously under irradiation especially in regions of high flaw density and that dielectrics charged up by irradiation can be discharged by micrometeorite impact at a later time.

Early work on discharges in irradiated dielectrics related the discharge to the sample material, the nature and quantum energy of the radiation, and the total exposure required to induce discharge. Empirical guidelines have been used by persons wishing to make Lichtenberg figures based on what worked in the past. A change in the radiation beam energy or the sample size or shape often resulted in no discharges but explanations for such effects were not quantitatively investigated. Only recently has some basic data and modelling become available to quantitatively predict the generation of intense electric fields in irradiated dielectrics (refs. 7-9).

From work in the various subfields of radiation transport (photon, proton, ion, electron, and neutron) we can predict the spatially dependent flux and current of charged particles at high energies (>100 eV) in the dielectric (ref. 10). Thus we can predict the spatial distribution of charge deposited by the high energy radiations. This distribution of charge can then be used to predict the electric fields internal to the dielectric.

Simultaneously, the problem of electric conduction in irradiated dielectrics has been theoretically (ref. 11) and experimentally (ref. 12) investigated. Results from these investigations allow us to calculate the conduction currents and the relaxation currents arising from the space charge fields in the dielectrics. It turns out theoretically, as we see below, that the conduction processes can either cause or prevent the development of breakdown fields. Information (ref. 13) and discrepancies (ref. 12) in the literature indicate that a great amount of uncertainty accompanies the evaluation of dielectric conductivity. However enough data exist that we can use it either as first guesses in our calculations or as worst case extremum in calculations for engineering application.

We can apply the radiation transport data and the dielectric conductivity data to Maxwell's equations and predict the transient or steady state response of a system of conductors and dielectrics. It is particularly simple in one dimension (ref. 14) although I believe we are constrained to numerical solutions on the computer in any case. We perform such a one-dimensional (1-D) calculation in this paper to illustrate the generic effects and the important parameters which relate to the bulk dielectric breakdown problem.

The particular example we choose to look at is dictated by availability of data on radiation transport, availability and ease of experimental comparison, possible application to spacecraft situations, and clarity of illustration. We irradiate thick (0.1 to 0.4 cm) sheets of Teflon with 1 MeV electrons while both sides of the sheet are at ground potential.

MODEL

The sample and irradiation geometry are shown in figure 1. The front and rear electrodes are assumed to not perturb the radiation transport in the dielectric; the amount of perturbation can be calculated and is truly negligible in this arrangement with electrons (ref. 15). The front electrode must be very

thin relative to an electron range and the rear electrode must be similar in atomic number to the dielectric. If the electrodes violate these constraints it is possible to correct "exactly" for the effect by use of electron transport codes but that involves extra work not related to the problem at hand.

For most of the calculations presented below, the Teflon was 0.3 cm thick. It has sometimes been found that breakdown occurs more readily in samples between one and two electron ranges thick and thus the choice of 0.3 cm. Results for other thicknesses are also given to show that theory similarly predicts such a thickness dependence.

The irradiation intensity may be high for spacecraft purposes but is chosen to correspond to easily realizable experimental conditions. Calculations have been made for various intensities, and nonlinearities which are due to dark conductivity effects do not become important until the intensity is reduced by 10^3 or more. For purposes of demonstration only we wish to avoid these effects.

Grounding or fixing the bias on both electrodes makes an immediately tractable situation. If we allowed the front surface to float, the calculation would become more complicated without improving our understanding. Because of (a) secondary emission effects, (b) the simultaneous presence of positive and negative charge plasma around the satellite, and (c) photoelectron emission, it seems that usually a dielectric surface will not charge beyond 10^4 volts relative to the rear electrode (body of the satellite). It is clear from the results that 10^4 volts on the surface will not significantly alter the large internal fields generated in the dielectric. Thus, grounding both electrodes is not expected to deviate from the situation seen on real satellites within the dielectric except in unusual cases.

The equations and numerical techniques have been completely described elsewhere (ref. 7). The dielectric is initially net charge neutral. The irradiation begins at time $t = 0$ and continues uninterrupted. As electrons accumulate in the dielectric, electric fields build up resulting in the generation of significant conduction current. The conduction current also causes charge to be moved around and deposited in the dielectric. This is a dynamic process which continues to change dramatically as the irradiation progresses in time.

At selected times we can use the computer print-out to monitor the spatial charge density, electric field, net current density (sum of incident electron beam current and conduction current) and meter current. The meter current is mathematically determined by integrating the net current density over the thickness of the dielectric: it can be thought of as the image current flowing to the rear electrode so that the electrode remains at ground potential. As we watch the various quantities change during the irradiation we can understand the physics of the process.

It is instructive to vary the parameters which describe the dielectric or the radiation and see the resulting changes. This provides further insight into the complex physical processes which take place. As in all numerical

solution techniques it is difficult to pick out the parameters, a-priori, that are critical to our situation. However, with a few runs given below we can see that certain parameters are important to the spacecraft charging problem.

RESULTS

The Calculation

Figure 2 describes the current directly attributable to the motion of the incident electrons as they scatter and lose energy in the dielectric; notice they are all stopped before penetrating 0.25 cm. This curve is an approximate fit to Monte Carlo data (ref. 17) using the function $A \exp(1 - \exp Bx^n)$ and is open to argument since very little data is available. However the shape is essentially correct and should serve our purposes well.

We calculate the rate of charge deposited by this high energy electron current from the continuity equation

$$-\frac{\partial \rho}{\partial t} = \frac{d\bar{J}}{dx} \tag{1}$$

in one dimension where ρ is the charge density, J is the current density, and x is the depth in the dielectric. We then determine $\rho(t)$ from

$$\rho(t) = \rho(t = 0) + \int_0^t \frac{\partial \rho}{\partial t'}\, dt' \tag{2}$$

Figure 3 shows the result for $t = 6$ seconds.

We can use several methods (Gauss' law is sufficient) to determine the electric field resulting from such a space density. The electric field resulting from the space charge density at $t = 6$ seconds is shown in figure 4. Note that peak fields are rapidly approaching 10^5 V/cm. Such large fields must result in some conduction current.

There are many many models we can use to estimate the conduction currents (ref. 13). Our purpose is not to validate conduction models but to investigate the parameters controlling field build-up in irradiated dielectrics. We choose to use a popular expression for conductivity (refs. 12,13)

$$\sigma = k\dot{D} + \sigma_0 \tag{3}$$

where σ is conductivity, k is a coefficient empirically determined (ref. 12), $\dot{D}$ is dose rate supplied by the high energy radiation, and σ_0 is the conductivity under no irradiation. Of course there are many other conductivity effects (field dependence, trap effects, total dose effects) which could be put easily into the computer but they do not help clarify the basic picture. Figure 5 is a plot of equation (3) for the particular case at hand (ref. 18); the

conductivity is a strongly varying function of depth in the dielectric.

Using the conductivity and electric field data we calculate the conduction current

$$\bar{J}_c(x) = \sigma(x)\bar{E}(x) \tag{4}$$

and assuming the high energy electron current, J_0, remains constant we determine the net current in the dielectric, J, from

$$\bar{J}(x,t) = \bar{J}_c(x,t) + \bar{J}_0(x) \tag{5}$$

Equations (1) and (2) are recalculated at time t using equation (5) to determine the electric field which results in a changed J_c and the process is continued, self consistently, using small time steps on the computer.

Data

Figure 6 shows the evolution of $J(x)$ from $t = 0$ to $t = 100$ seconds; there is quite a change occurring in $J_c(x)$ over this time span as a result of the build-up of spacecharge. Figure 7 shows the spacecharge density from $t = 0$ to $t = 100$ seconds. The increase in magnitude of ρ as the irradiation progresses is a natural result of the deposition of high energy electrons. The drastic change of shape between $\rho(x,t = 10)$ and $\rho(x,t = 100)$ curves is a dramatic demonstration of the importance of conduction currents. Figure 8 shows the evolution of $E(x)$ from $t = 0$ to $t = 100$ seconds. Notice that $E(x)$ is approaching maximum values of 10^6 V/cm which may cause breakdown.

Figure 9 describes the net current density, $J(x)$, for times from 100 to 500 seconds. Notice that as time progresses, the current density is tending towards a "flat" function. If $J(x)$ were constant then $\partial\rho/\partial t$ would be zero. It is postulated here that <u>usually</u> the build-up of conduction current occurs in such a way that $J(x)$ becomes, ultimately, a constant and final equilibrium is obtained. However irradiation and geometrical conditions might be obtainable so that oscillatory equilibrium occurs (for example analogous to the Gunn effect (ref. 19)).

Also notice in figure 9 that the "peak" is continually moving to the right. This has important implications for the electric field build-up near the rear electrode. The motion of this "peak" is very dependent on the assumed initial current distribution, $J_0(x)$, especially in the region of large x. It should be noted that in this region of x, $J_0(x)$ is sometimes called the straggling tail of the electron penetration distribution and is a subject of current controversy; the exact shape of the curve for $J_0(x)$ at large x is uncertain and yet may have importance in this dielectric area. At late times in the irradiation, only electrons in this straggling tail region penetrate the dielectric beyond the centroid of the spacecharge distribution and contribute to a continuing change in the spacecharge density. MeV electrons which do not penetrate to the "peak" at late times are exactly cancelled by conduction processes at these shallower depths.

Figure 10 plots the spacecharge density $\rho(x)$, at times from 100 to 1000 seconds. Notice that the peak in electron density constantly moves to larger depths as the electrons in the straggling tail become caught between the repulsive force of the charge distribution centroid and the "impenetrable" region of low conductivity near the rear electrode. An important concept results from this: If a region of negligible conductivity exists, the $J_0(x)$ distribution may cause continued spacecharge build-up until the spacecharge fields are comparable to the free electron stopping power of the medium which usually exceeds 10^7 V/cm - a field definitely in the breakdown category.

Also notice in figure 10 the important result that a positive spacecharge density develops in the region of $x = 0.12$ cm. This is similar to a result experimentally observed by Evdokimov and Tubalov (ref. 20) and theoretically predicted by Matsuoka et al. (ref. 9) by a similar calculation. The positive spacecharge has important implications for the spacecraft charging problems. The process which generates the positive spacecharge might be described as follows:

(a) A large negative spacecharge occurs near the extrapolated range depth of the incident electrons.

(b) The resulting electric field drives carriers through the conducting regions, such carriers then pile up at the borders of the less-conductive regions.

(c) In this case, "holes" are driven from the region of high dose rate (where they are generated) towards the negative charge centroid. Before they reach the negative charge region they are "stopped" by the significantly lowered conductivity (at approximately 0.15 cm) near the negative charge centroid. (This argument is for qualitative purposes and is not meant to imply that either holes or electrons are the dominant conduction mechanism.)

Figures 11 and 12 show how the net current density continues to decrease on average, continues to "flatten out" and how the electrons in the straggling tail continue to add electrons deep in the dielectric. The curves have not been computed for $t > 5\times10^4$ seconds but it is obvious that straggling electrons will continue to add charge until the conduction through the unirradiated region, $J_c(x = 0.3$ cm), equals the net current at the front surface $J(x = 0)$.

Figure 13 describes the space charge density as time progresses out to 5×10^4 seconds. The trends evident in prior figures continue but we are now approaching equilibrium. Another important fact becomes obvious for electron irradiated dielectrics: For fully penetrating radiations such as thin dielectrics or gamma rays equilibrium is reached at total doses typically 10^5 rads or less (ref. 12) but for nonpenetrating radiations the straggling effect can substantially increase the "dose to equilibrium," in this case to greater than 10^7 rads.[1] It should be noted that Teflon seriously degrades at 10^6 rads while most other dielectrics require 10^8 or more for degradation.

[1] $(5\times10^4$ seconds) $(2\times10^2$ rads/sec) $= 10^7$ rads.

Figure 14 is a plot of the electric field at late times. Notice that the field $E(x = 0,t)$ has stabilized while at $x > 0.1$ it has not stabilized. The electric field is the most important parameter since we are interested in predicting breakdown. There are three maxima in the field; at the front surface, at the rear surface, and at approximately 0.18 cm. In one dimension the front and rear surface fields are derivable from the zeroth and first moments of the charge distribution (i.e., from the net total charge and the position of the centroid of the charge) but the fields interior to the dielectric are calculable only from the full distribution. At late times the field interior to the dielectric (related to the positive space charge region) becomes larger than the front surface field and also of sufficient magnitude to produce breakdown.

It should be remembered that the positive space charge region resulted from the conductivity gradient. We can generalize this result to say that any dielectric structure with a conductivity gradient is likely to internally charge up to produce large electric fields in regions adjacent to the gradient while under external irradiation. If one constructs a dielectric of layers (even of the same material from different batches) one is introducing another mechanism whereby dielectric breakdown under irradiation might occur. Conductivity gradients can be introduced by many factors (heat and light, for example) and should be avoided in spacecraft dielectrics.

Figure 15 is a plot of the three maxima in the electric field as a function of time. Of course these results are peculiar to the particular conditions chosen for this exercise. The relative magnitudes of the maxima (peaks) could change severely with changes in sample thickness, beam energy, dark conductivity, or coefficient of induced conductivity k (see eq. (3)). Other terms such as delayed conductivity, field dependent conductivity, and radiation damage would also be important. Never-the-less this figure vividly demonstrates that breakdown fields can occur with greatest likelihood near the surfaces or in interior regions of modulated conductivity.

The dark conductivity σ_0 assumed in the calculations was 10^{-20} ohm^{-1} cm^{-1}, probably an extreme for "Teflon." Similar calculations were also run for $\sigma_0 = 10^{-17}$ ohm^{-1} cm^{-1}, the other extreme, with almost identical results. The main difference is obvious in figure 15: the interior and rear surface field strengths do not become quite as large and reach equilibrium sooner.

Teflon has a coefficient of induced conductivity k greater than most dielectrics of interest. If we decrease k then the equilibrium electric fields will increase and thus other dielectrics are more likely than "Teflon" to breakdown. They may easily build up fields 10 times higher than Teflon in some irradiation conditions.

We can vary the coefficient of radiation induced conductivity by a factor of 10 or more and still be within the range of values reported in the literature. Table 1 describes the results for one particular case. Notice that the coefficient of induced conductivity acts nearly as a dark conductivity term at the front surface, that is, the electric field is nearly linearly dependent on resistivity, but at the center and rear the fields are not linearly dependent on the coefficient. This nonlinearity is strong when the radiation is nonpene-

trating. With fully penetrating radiation the equilibrium electric fields are always nearly linearly dependent on the coefficient of radiation induced conductivity.

It is interesting to vary the dielectric thickness and see how the three maximum (peak) field strengths vary. Table 2 shows the results for 1 MeV electron irradiation. In general, fully penetrating radiation is likely to produce smaller fields than nonpenetrating radiation and Bernhard Gross reports experiments on electron irradiations where breakdowns indeed occur most readily in samples with thicknesses between one and two electron ranges. However, by no means are breakdowns exclusive to this thickness range.

COMPARISON WITH EXPERIMENT

Our calculations produce one easy observable - the meter current. Figure 16 shows the meter current as a function of time during the irradiation. We have not been able to do the experiment prior to this conference but a similar experiment and calculation has been reported (ref. 9) with excellent agreement. Considering all the variables and their uncertainties, I would not expect good agreement in general. For several years we have been performing similar experiments with γ and X-rays without obtaining (meter current) excellent agreement, but we have created large fields routinely - it is a shocking experience to handle an irradiated dielectric.

This experiment has been performed once since the conference with poor comparison with the theory. The meter current was two orders of magnitude lower than expected at early time so we raised the beam current intensity to 4×10^{-4} A/m^2. The current slowly rose in time starting at 2×10^{-8} A and 3000 seconds later was 2.7×10^{-7} A declining to 1.3×10^{-7} A by 10^4 seconds. After 3000 seconds the meter began violent, sometimes full scale pulsing reflecting some sort of breakdown process which grew throughout the remaining irradiation. This irradiation was significantly more intense than the calculations above, but such an effect would not be predicted by the model.[2]

There are methods for investigating the trapped charge distribution in the dielectric such as thermally stimulated discharge and others (ref. 20), but the methods are indirect and may contain weak assumptions. This area seems to be more popular in the recent literature. I hope further work in this area will prove helpful to us. We would like to do similar calculations for a broad spectrum of irradiations but it will be hard work to put together a dose profile for 1 keV to 10 MeV electrons from the literature; it will be impossible to find data to construct the high energy electron current profile for that energy range. The best we could do is to make a guess or to get "someone" to do a Monte-Carlo run for a specific spectra of interest. Based on experience from several tens of calculations (refs. 7,12) for a variety of materials under a variety of irradiations I believe that for any given spectrum with quanta above

[2]Immediately prior to publication a lower intensity experiment was performed and gave agreement with the model at early times. The reason for the above discrepancies is not yet clear.

10 keV large fields will be generated in most "good" dielectrics and that given a particular dielectric geometry it is the unusual spectra which would not substantially charge dielectrics. I think it would be unlikely to find a spectra which would not charge a dielectric to $>10^5$ V/cm; further work is required to prove or disprove this statement (ref. 21).

It is here proposed that the following experiment be done because it is central to spacecraft charging. The theory described above can predict values for radiation induced conductivity and dark conductivity which would significantly reduce the maximum electric fields. We know that nonpenetrating high energy electrons are as troublesome as any radiations so we could alter samples to increase k and σ_0 and use electrons to test their charge-up response. It may be possible to formulate dielectrics with the proper spacecraft properties (optical, thermal, mechanical as well as conductive) without the danger of field build-up.

It is clear that effects such as field dependent conductivity, dose related damage, radiation induced traps, contacts, etc., can be important. They all impact the generation of fields through the conductivity term in our model. Their quantitative evaluation is very variable for materials of interest. At this time, such effects seem to be relatively small compared to the radiation induced conductivity term. But, it might be profitable to consider these effects with an eye to increasing the conductivity under irradiation and through the unirradiated region, if any exists. Experiments on these effects would be helpful.

SUMMARY

We have described a model which predicts currents and fields in irradiated dielectrics; we find some weak empirical agreement in the literature and in our own experiments. It turns out that the parameters which describe the conduction mechanisms in the dielectric may be critical for spacecraft purposes since they seem to be the handle by which we can prevent excessive electric field build-up. A nonuniform conductivity profile in the dielectric is shown to be potentially important: we should avoid such profiles. In general the higher energy quanta (>10 keV) are probably more important because they penetrate deeper and deposit greater electric potential energy in the dielectric causing more energetic breakdown discharges.

Several suggestions are made concerning the search for usable dielectrics which will not substantially charge up; increasing the bulk conductivity offers the greatest potential for eliminating discharges and decreasing differential charging.

REFERENCES

1. Furuta, J., Hiraoka, E., and Okamoto, S., J. Appl. Phys. 37, 1873 (1966).

2. Vorob'ev, A. A., Zavadovskaya, E. K., Starodubtsev, V. A., and Fedorov, B. V., Soviet Physics Journal, 1977, Plenum Press, translator, p. 171. (UDC 53.043:537.224).

3. Brown, R. G., J. Appl. Phys. 38, 3904 (1967).

4. Evdokimov, O. B., Kononov, B. A., and Yagushkin, N. I., Soviet Physics Journal 1978 (Plenum Press translation), p. 1339.

5. Zavadovskaya, E. K., Annenkov, Yu. M., Starodubtsev, V. A., Vakhromeev, V. G., and Malofienko, G. M., Soviet Physics Journal (Plenum Press translation) 1974, p. 144.

6. Gross, B., Dow, J., and Nablo, S. V., J. Appl. Phys. 44, 2459 (1973).

7. Frederickson, A. R., AFCRL-TR-74-0582, 1974 (Available NTIS); IEEE Trans. Nuc. Sci. NS22, 2556 (1975).

8. Pigneret, J., and Strobak, H., IEEE Trans. Nuc. Sci. NS23, 1886 (1976).

9. Matsuoka, Shingo, et al., IEEE Trans. Nuc. Sci. NS23, 1447 (1976).

10. High energy radiation transport modeling has steadily improved since 1950 with the widespread use of nuclear energy. For example, data for the calculations below was obtained from work by Martin Berger of NBS during the 1960's and from work by John Halbleib et al. of Sandia Labs. during the 1970's. Many other sources for such data are now available in the literature.

11. No single reference is helpful here. To appreciate the diversity of this field, one must review a large number of works and the following brief list of authors is a beginning point: Albert Rose (book), Richard H. Bube (book), J. F. Fowler, H. J. Wintle, Bernhard Gross, Thomas J. Ahrens, L. K. Monteith, and H. E. Boesch.

12. For a reasonably complete up to date listing of references see A. R. Frederickson, IEEE Trans. Nuc. Sci. NS24, 2532 (1977). For a list of parameters for various dielectrics see T. J. Ahrens and F. Wooten, IEEE Trans. Nuc. Sci. NS23, 1268 (1976), and R. C. Weingart et al., IEEE Trans. Nuc. Sci. NS19, 15 (1972).

13. Wintle, H. J., IEEE Trans. Electrical Insulation, EI-12, 97-113 (1977). Also contains extensive references.

14. For an example of the increased complexity of modeling in 3-D see I. Katz et al., NASA CR-135256, "A Three Dimensional Dynamic Study of Electrostatic Charging in Materials" (Aug. 1977).

15. However if we were using X-ray irradiation, the choice of electrodes could severely distort the results as is shown in references 7, 8, and 16.

16. Chadsey, W. L., IEEE Trans. Nuc. Sci. NS21, 235-42 (1974).

17. Perkins, J. F., Phys. Rev. 126, 1781-4 (1962).

18. For examples of dose depth data see: G. J. Lockwood, G. H. Miller, and J. A. Halbleib, IEEE Trans. Nuc. Sci. NS20, 326 (1973); Harvey Eisen, "Electron Depth-Dose Distribution Measurements in Metals and Two Layer Slabs" Thesis, Univ. Maryland, Dec. 6, 1971; M. J. Berger and S. M. Seltzer, Protection Against Space Radiation, NASA SP-169, p. 285 (1967).

19. Private communication, Jacques E. Ludman, 1978.

20. Evdokimov, O. B., and Tubalov, N. P., Sov. Phys. Solid State 15, 1869 (March 1974, A.I.P. Translation).

21. Similar calculations for ∿10 keV electrons are reported by Beers and Pine at this conference and their results seem to be in agreement with these comments.

TABLE 1. - PEAK ELECTRIC FIELDS AT EQUILIBRIUM FOR 0.24-cm-THICK TEFLON UNDER 1-MeV ELECTRONS FOR THREE ASSUMED VALUES OF k [10^{-5} A/m^2; $\sigma_0 = 10^{-17}$ ohm^{-1}cm^{-1}.]

k (see eq.(3)) sec/ohm meter rad	Equilibrium Electric Field Intensity, V/cm		
	Front	Center	Rear
10^{-14}	.056	.047	.52
10^{-15}	.545	.40	2.78
10^{-16}	4.81	2.42	10.2

TABLE 2. - PEAK ELECTRIC FIELD INTENSITIES AS FUNCTION OF "TEFLON" THICKNESS FOR ASSUMED VALUE OF DARK CONDUCTIVITY [$\sigma_0 = 10^{-17}$ ohm^{-1}cm^{-1}; k = 10^{-15}.]

Dielectric Thickness	Equilibrium Field, 10^6 V/cm		
	Front	Center	Rear
.10 cm	.069	not defined	.108
.15 cm	.221	not defined	.639
.18 cm	.375	(.12)	1.71
.20 cm	.466	.20	2.76
.22 cm	.521	.31	3.34
.24 cm	.545	.40	2.78
.30 cm	.559	.50	1.04

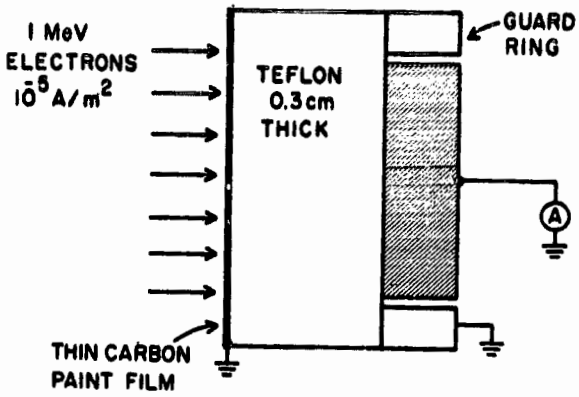

Fig. 1. The apparatus being modeled in the calculations and constructed for experimental comparison.

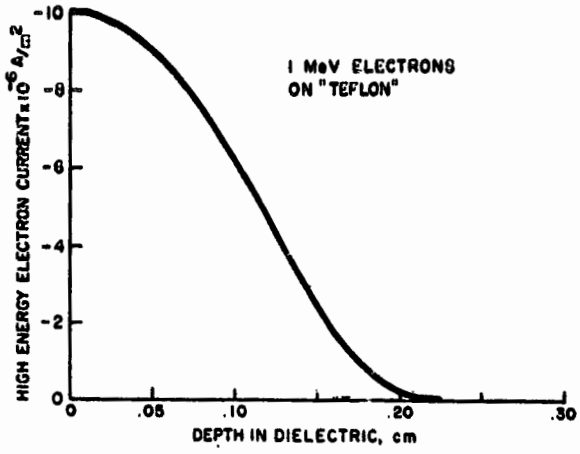

Fig. 2. The electric current due directly to the incident high energy electrons.

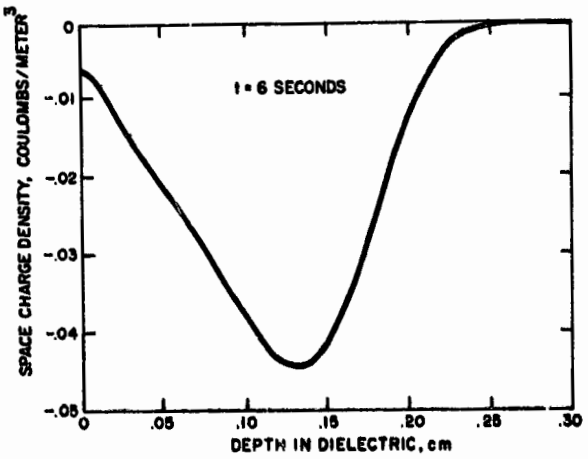

Fig. 3. The charge deposited in the dielectric by the current profile in figure 2 after six seconds irradiation.

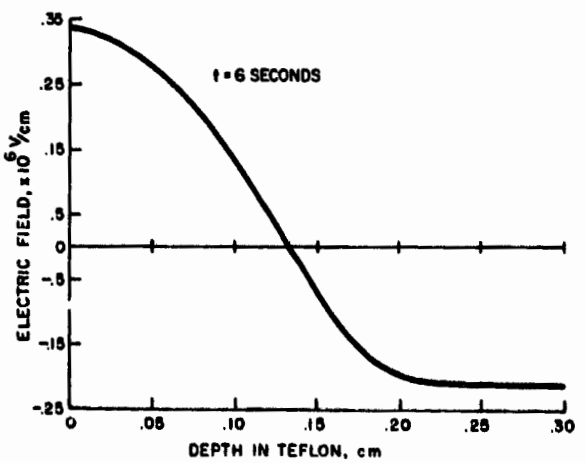

Fig. 4. The electric field due to the space charge shown in figure 3.

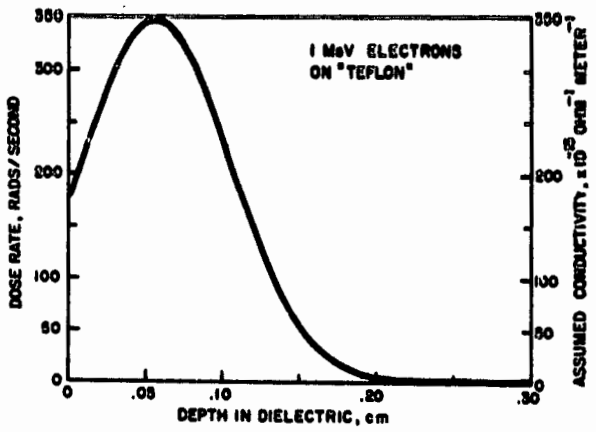

Fig. 5. The dose profile due to the irradiation. The conductivity profile is obtained from equation (3) using values for k obtained from reference 12.

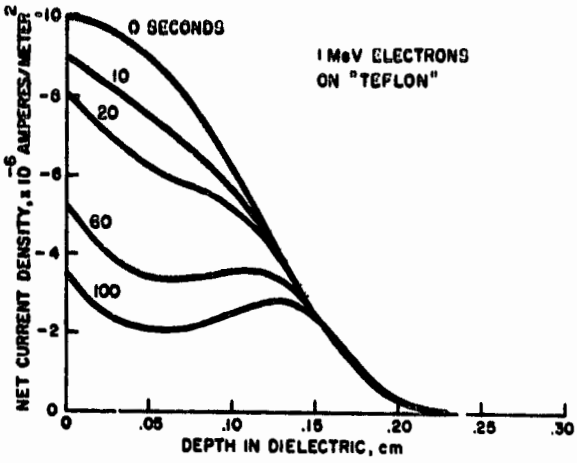

Fig. 6. The evolution of net current density (eq. (5)) at early times.

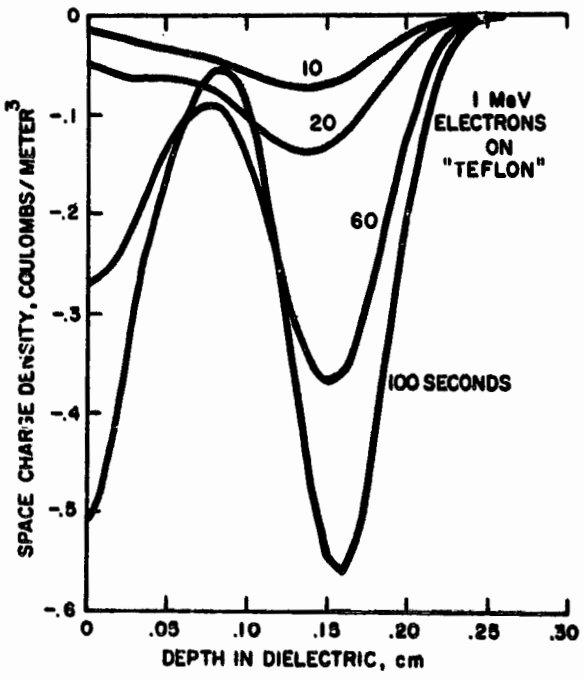

Fig. 7. The evolution of space charge density (eq. (2)) at early times.

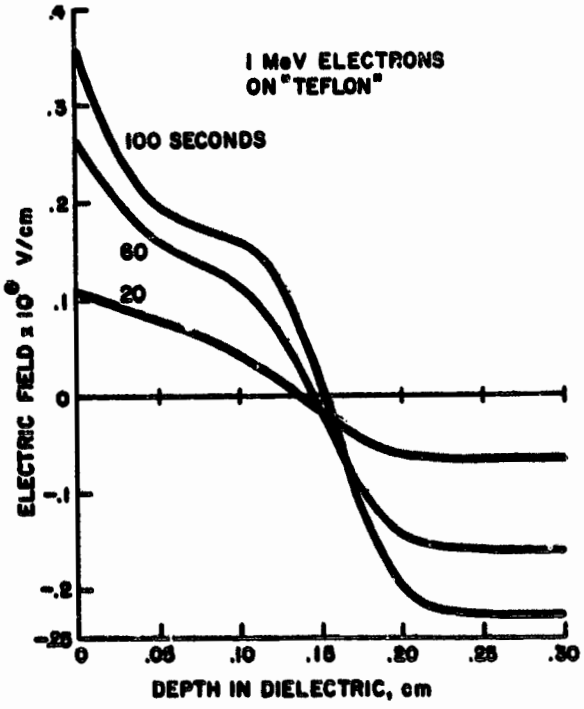

Fig. 8. The evolution of electric fields at early times.

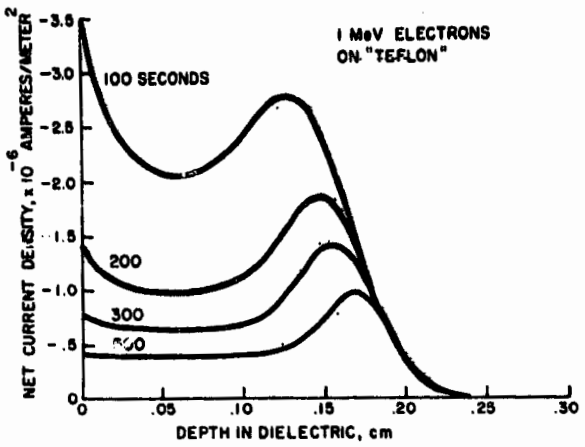

Fig. 9. The evolution of net current density at later times, 100 to 500 seconds.

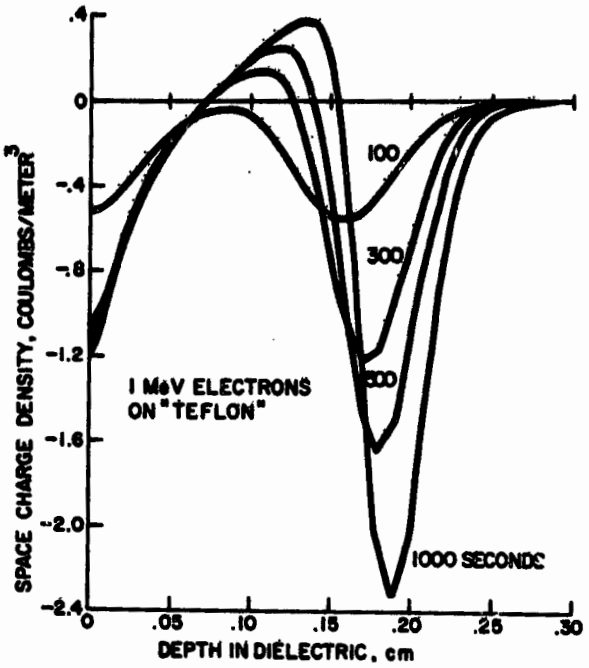

Fig. 10. Space charge density at times from 100 to 1000 seconds.

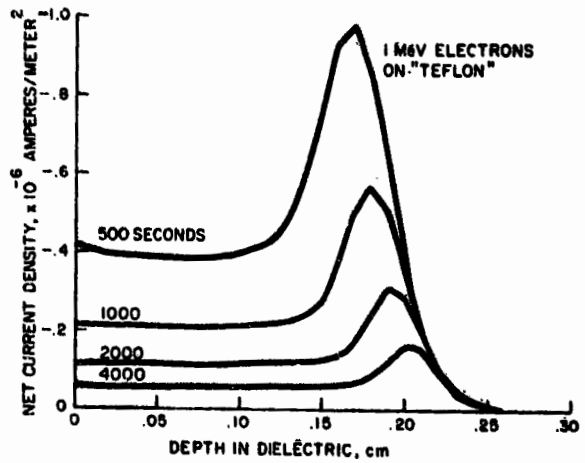

Fig. 11. Net current density at times from 500 to 4000 seconds.

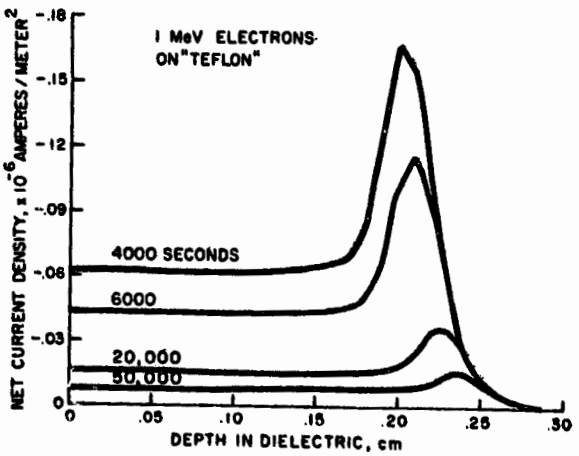

Fig. 12. Net current density at times 4000 to 50,000 seconds.

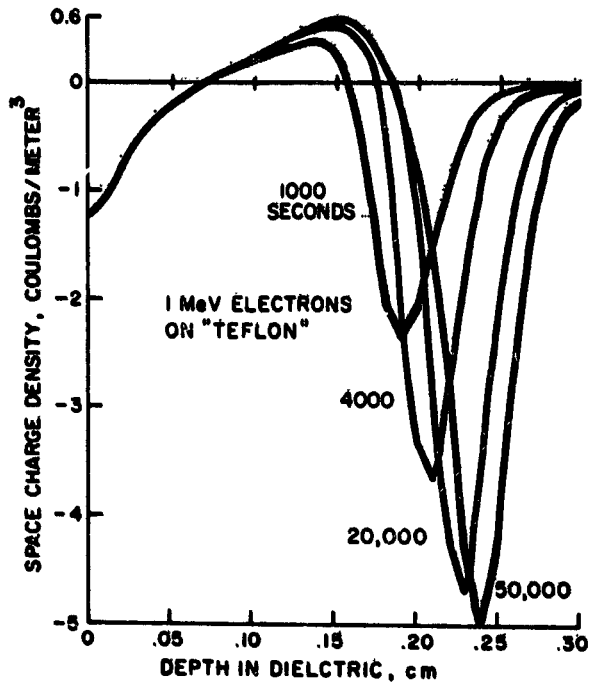

Fig. 13. Space charge density at times from 1,000 to 50,000 seconds.

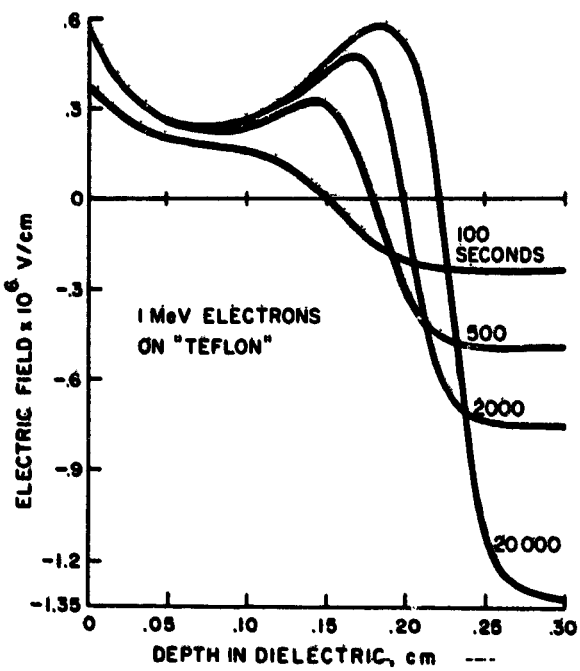

Fig. 14. Electric field at late times, 100 to 20,000 seconds.

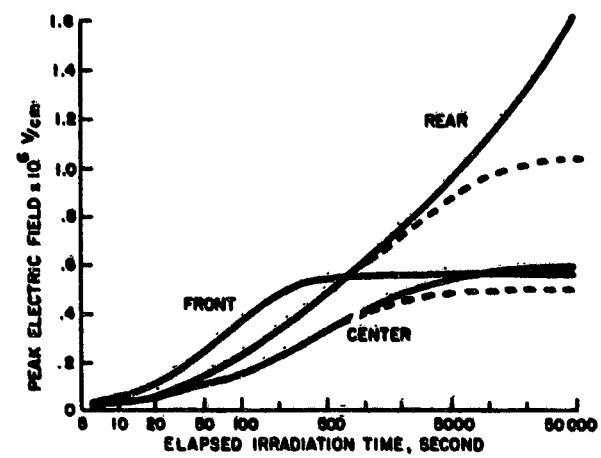

Fig. 15. Electric field intensity maxima for the three peaks evident in figure 14. The solid lines are for dark conductivity $\sigma_0 \cdot 10^{-20}$ ohm^{-1}cm^{-1}, the dashed lines for $\sigma_0 \cdot 10^{-17}$ ohm^{-1}cm^{-1}.

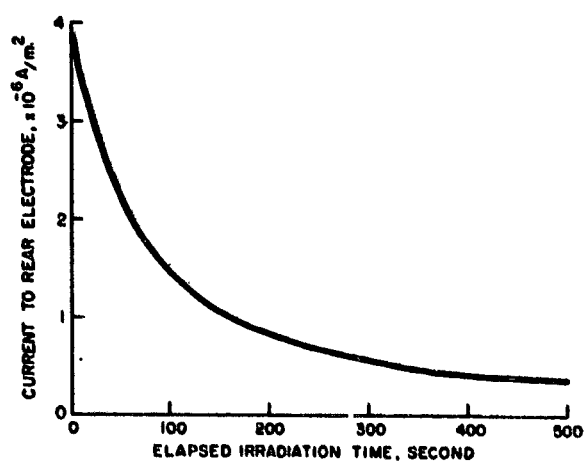

Fig. 16. Ammeter current as a function of time: see figure 1.